Real-time *in vivo* mitochondrial redox assessment confirms enhanced mitochondrial reactive oxygen species in diabetic nephropathy

Daniel L. Galvan[1], Shawn S. Badal[1], Jianyin Long[1], Benny H. Chang[2], Paul T. Schumacker[3], Paul A. Overbeek[2] and Farhad R. Danesh[1,4]

[1]*Section of Nephrology, The University of Texas MD Anderson Cancer Center, Houston, Texas, USA;* [2]*Department of Molecular & Cell Biology, Baylor College of Medicine, Houston, Texas, USA;* [3]*Department of Pediatrics, Feinberg School of Medicine, Northwestern University, Chicago, Illinois, USA; and* [4]*Department of Pharmacology, Baylor College of Medicine, Houston, Texas, USA*

While increased mitochondrial reactive oxygen species have been commonly implicated in a variety of disease states, their *in vivo* role in the pathogenesis of diabetic nephropathy remains controversial. Using a two-photon imaging approach with a genetically encoded redox biosensor, we monitored mitochondrial redox state in the kidneys of experimental models of diabetes in real-time *in vivo*. Diabetic (*db/db*) mice that express a redox-sensitive Green Fluorescent Protein biosensor (roGFP) specifically in the mitochondrial matrix (*db/db*mt-roGFP) were generated, allowing dynamic monitoring of redox changes in the kidneys. These *db/db*mt-roGFP mice exhibited a marked increase in mitochondrial reactive oxygen species in the kidneys. Yeast NADH-dehydrogenase, a mammalian Complex I homolog, was ectopically expressed in cultured podocytes, and this forced expression in roGFP-expressing podocytes prevented high glucose–induced increases in mitochondrial reactive oxygen species. Thus, *in vivo* monitoring of mitochondrial roGFP in diabetic mice confirms increased production of mitochondrial reactive oxygen species in the kidneys.

Kidney International (2017) ■, ■–■; http://dx.doi.org/10.1016/j.kint.2017.05.015

KEYWORDS: diabetic nephropathy; mitochondria; podocyte; reactive oxygen species

Correspondence: *Farhad R. Danesh, Section of Nephrology, The University of Texas MD Anderson Cancer Center, 1400 Pressler Street, Unit 1468, Houston, Texas 77030, USA. E-mail: fdanesh@mdanderson.org*

Received 19 October 2016; revised 18 April 2017; accepted 4 May 2017

The mitochondrial dysfunction theory of microvascular complications of diabetes, outlined by Brownlee,[1] proposes that high glucose (HG)-induced mitochondrial reactive oxygen species (mtROS) production contributes to many features of microvascular complications of diabetes, including diabetic nephropathy (DN). A large body of evidence in experimental models of diabetes has corroborated this hypothesis.[2–4] However, a recent published work has disputed this theory.[5] Dugan *et al.* assessed superoxide production in the kidneys of experimental models of diabetes and reported a significant reduction in mitochondrial biogenesis in conjunction with decreased superoxide in the kidneys of diabetic mice.[6] These conflicting results on the role of mtROS in DN could be attributed to the central challenge of detecting and analyzing mtROS *in vivo*. To address this, we generated a mouse model to dynamically monitor mtROS *in vivo* by taking advantage of a reduction-oxidation sensitive green fluorescent protein (roGFP), specifically expressed in the mitochondrial matrix.[7] We generated transgenic roGFP diabetic mice by crossing our transgenic mice with an established model of DN mice (*db/db*), to generate a type 2 diabetic mouse model with a genetic mitochondrial-redox biosensor ($db/db^{\text{mt-roGFP}}$).

Redox-sensitive roGFP has been previously used to dynamically monitor redox status in real time *in vivo* under a variety of conditions.[8,9] To exclusively monitor redox changes in mitochondria, we targeted roGFP to the mitochondrial matrix (mt-roGFP) using the mitochondrial targeting sequence from cytochrome oxidase subunit IV.[7] The mt-roGFP reporter is sensitive to the oxidation status of glutathione (GSH/GSSG) in the mitochondrial matrix,[7–9] where the redox status can be detected by interrogating mt-roGFP at 2 wavelengths while measuring emission at a third wavelength.[8,9] This reporter offers several advantages. First, its exclusive expression within the mitochondrial matrix provides an organelle-specific readout of redox status within the cell. Second, oxidation of the sensor is reversible, allowing it to provide a continuous readout of the dynamic balance between oxidant generation and the effectiveness of thiol reducing capacity. Third, the ratiometric assessments are independent of expression levels and mitochondrial membrane potential.[9]

RESULTS

To monitor mtROS *in vivo*, we took advantage of a recently employed mouse model in which a CMV-driven, mitochondrial matrix–targeted redox-sensitive GFP is transgenically encoded (mt-roGFP).[7,9] Transgenic mt-roGFP mice were intercrossed with mice harboring the Lepr$^{db/+}$ mutation to generate a type 2 diabetic mouse model with a genetic redox biosensor (*db/db*$^{mt\text{-}roGFP}$). Generation of these transgenic mice enabled us to specifically monitor mtROS *in vivo* in the kidneys of diabetic mice.

We engaged 2-photon microscopy to monitor the mitochondria-specific redox status of roGFP in the kidneys of live, anesthetized mice (Figure 1a). The mt-roGFP biosensor was colocalized with mitochondrial markers *in vitro* and *in vivo* (Figure 1b and c). We next performed live imaging of kidneys in 8- and 16-week-old diabetic *db/db*$^{mt\text{-}roGFP}$ and nondiabetic *db/m*$^{mt\text{-}roGFP}$ mice. Representative 2-photon imaging revealed a marked increase in the fluorescent intensity of oxidized (red) mt-roGFP and a decrease in the fluorescent intensity of reduced (green) mt-roGFP in the kidneys of diabetic *db/db*$^{mt\text{-}roGFP}$ mice compared with *db/m*$^{mt\text{-}roGFP}$ mice (Figure 2a). Ratiometric analysis of both 8- and 16-week-old animals confirmed a significant increase in the proportion of oxidized roGFP in the kidneys of diabetic reporter mice (Figure 2b).

The 2-photon microscopy approach is limited in its ability to spatially delineate the contribution of glomerular versus nonglomerular compartments. To address this and to assess the levels of mtROS specifically in the glomeruli, we performed an *in situ* analysis to specifically visualize glomeruli by a systemic injection of dextran-TxRed (Figure 2c, left panels). As in live animals, representative images demonstrate enhanced mtROS in glomeruli and tubules in diabetic *db/db*$^{mt\text{-}roGFP}$ mice compared with control *db/m*$^{mt\text{-}roGFP}$ mice (Figure 2d, right panels). Quantitation of biosensor ratios indicated significant differences between diabetic and nondiabetic kidneys in both the glomerular and tubular regions (Figure 2e).

We then tested whether the observed increase in ROS could be mitigated by mitoTEMPO, a mitochondrial-targeted antioxidant, in diabetic *db/db*$^{mt\text{-}roGFP}$ mice. Using live-cell imaging, we assessed real-time redox changes in response to mitoTEMPO in cultured mouse podocytes exposed to HG conditions (25 mM). We observed that the HG-induced increases in mtROS were prevented with mitoTEMPO treatment (100 μM) (Figure 3a and b). We next examined the *in vivo* effect of mitoTEMPO on mtROS in the kidneys of diabetic *db/db*$^{mt\text{-}roGFP}$ animals. To this end, *db/db*$^{mt\text{-}roGFP}$ mice were administered mitoTEMPO for 3 days (10 mg/kg/d i.p.). Ratiometric analysis of the mitochondrial redox state demonstrated that diabetic *db/db*$^{mt\text{-}roGFP}$ mice treated with mitoTEMPO exhibited less mtROS compared with *db/db*$^{mt\text{-}roGFP}$ mice treated with vehicle (Figure 3c and d). The results are consistent with a previous report demonstrating attenuated key histological features of DN upon treatment with mitoTEMPO.[10]

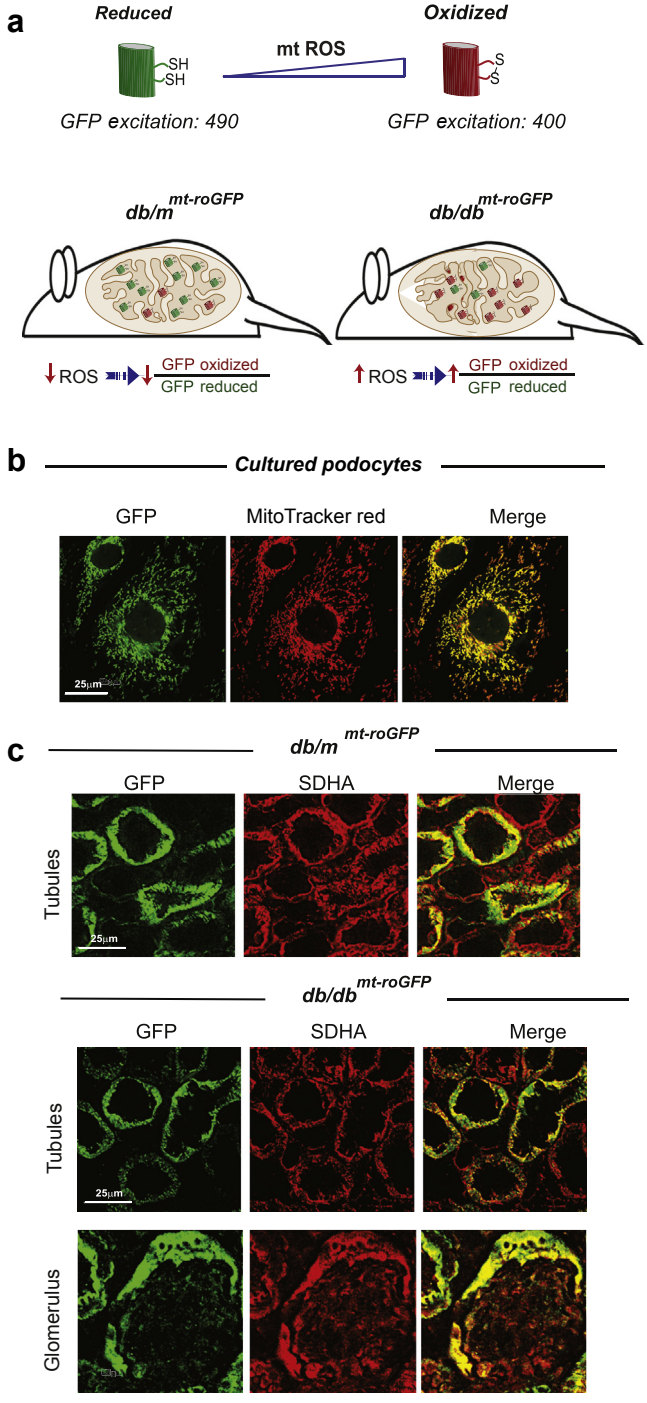

Figure 1 | Mitochondrial reduction/oxidation biosensor. (**a**) Schematic depiction of the mitochondrial redox-sensitive reduction-oxidation–sensitive green fluorescent protein (mt-roGFP). Disulfide formation of 2 cysteines promotes protonation of the chromophore increasing the excitation peak near 400 nm at the expense of the 490 nm peak. (**b**) Immunolabled GFP (left), MitoTracker red (middle) and merged images (right) show colocalization in cultured podocytes. (**c**) Frozen section from 8-week-old *db/m*$^{mt\text{-}roGFP}$ (top panels) and *db/db*$^{mt\text{-}roGFP}$ mouse kidneys (lower panels) are shown. Immunolabled GFP fluorescence (left), immunolabled succinate dehydrogenase subunit A (SDHA; middle), and merged images (right). Diabetic *db/db*$^{mt\text{-}roGFP}$ kidney sections from both tubular and glomerular regions are displayed. mtROS, mitochondrial reactive oxygen species. To optimize viewing of this image, please see the online version of this article at www.kidney-international.org.

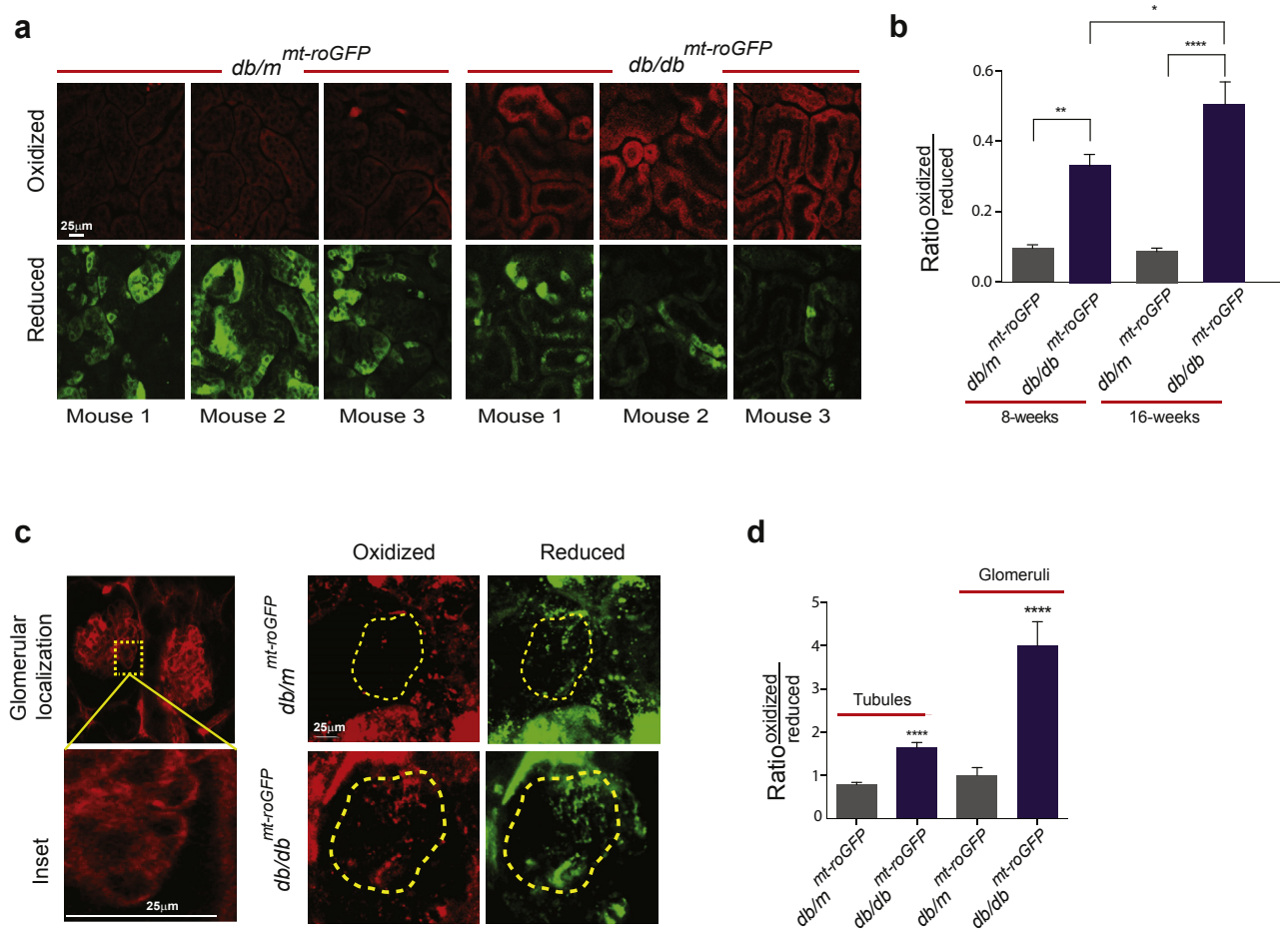

Figure 2 | Kidneys in live diabetic mice display increased mitochondrial reactive oxygen species production. (**a**) Two-photon live imaging of control (*db/m*$^{mt\text{-}roGFP}$, left) and diabetic (*db/db*$^{mt\text{-}roGFP}$, right) 16-week-old mouse kidneys. Top panels display images from the oxidized excited sensor (400 nm), while the bottom are the reduced sensor (490 nm). (**b**) Quantification of the excitation ratios determined from 2-photon images of *db/m*$^{mt\text{-}roGFP}$ and *db/db*$^{mt\text{-}roGFP}$ animals at 8 and 16 weeks of age. Bar = 25 μm. (**c**) Representative *in situ* confocal images of kidney slices from control mice administered TxRed-Dextran (70 kD, left). Confocal images taken from *in situ* kidney slices displaying the oxidized and reduced signals (right). Yellow-dashed inscribed area denotes glomerular region determined with TxRed. Bar = 25 μm. (**d**) Quantification of excitation ratio signal from *in situ* images. On the left are ratios from regions outside of the inscribed area, labeled tubules. On the right are ratios from the inscribed area labeled glomeruli. Data are presented as mean ± SEM. *$P < 0.05$, **$P < 0.01$, ****$P < 0.001$. mt-roGFP, mitochondrial reduction-oxidation–sensitive green fluorescent protein. To optimize viewing of this image, please see the online version of this article at www.kidney-international.org.

Mitochondrial respiratory chain dysfunction is one mechanism implicated in increased mtROS and has been associated with microvascular complications of diabetes.[3,11–15] We speculated that complex I (NADH-quinone oxidoreductase) may play a key role as a source of mtROS, as suggested in a previous study.[16] We observed that complex I activity was markedly reduced in mitochondria harvested from podocytes of *db/db* mice compared with podocytes from control mice (Figure 4a). We hypothesized that if complex I dysfunction contributes significantly to mtROS in the HG milieu, circumventing complex I could potentially attenuate enhanced mtROS in HG conditions. Toward this end, we employed a well-characterized NADH dehydrogenase, Ndi1, from *Saccharomyces cervisiae*.[17,18] The yeast Ndi1 protein has been shown to rescue complex I dysfunction by facilitating electron transport from NADH to coenzyme Q without proton pumping and production of mtROS (Figure 4b).[19] To test whether Ndi1 attenuates mtROS in HG conditions, we stably transfected cultured podocytes with mt-roGFP and a cDNA expression plasmid encoding Ndi1. Successful expression of mRNA for both constructs was confirmed in cultured podocytes (Figure 4c). Functional expression of Ndi1 was confirmed by demonstrating that podocytes became resistant to respiratory inhibition by rotenone (1 μM), which inhibits mammalian complex I but not Ndi1 (Figure 4d). Dose response curves identified an IC_{50} of 617nM for Ndi1 expressing podocytes versus 407nM for controls (Figure 4d). Live cell imaging of stably transfected mt-roGFP/Ndi1 cultured podocytes exposed to HG indicated that HG-induced increases in mtROS were prevented in podocytes expressing Ndi1 (Figure 4e and f). We found similar results in a mouse renal tubular epithelial cell line

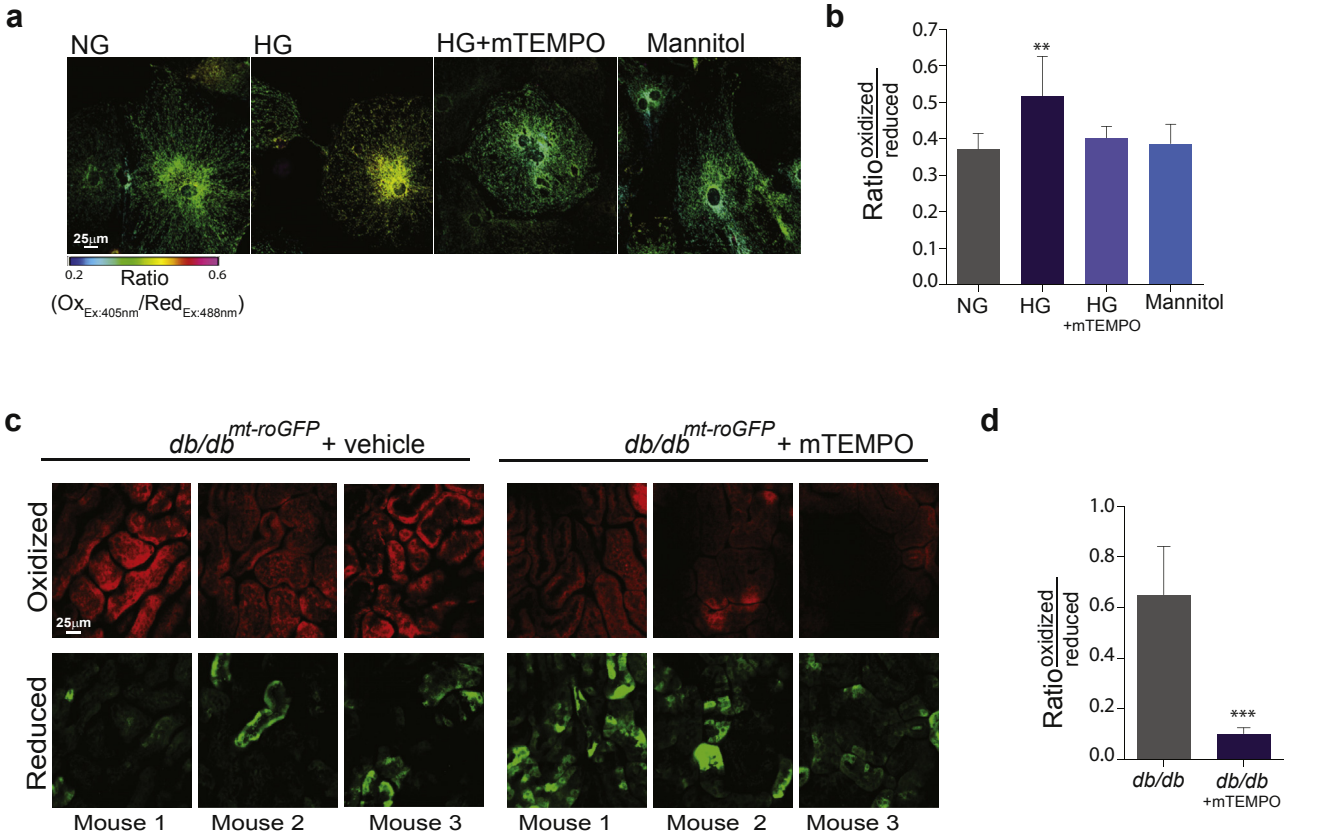

Figure 3 | Treatment with mitoTEMPO ameliorates high glucose (HG)-induced mitochondrial reactive oxygen species *in vitro* and *in vivo*. (**a**) Pseudocolored ratiometric images of podocytes cultured in normal glucose (NG; 5 mM), HG (25 mM), HG with 100 μM mitoTEMPO, or 25 mM mannitol for 48 hours. Images shown as gradient of color intensity from the more reduced (blue) form to the more oxidized (purple) form of mitochondrial reduction-oxidation–sensitive green fluorescent protein (mt-roGFP). Bar = 25 μm. (**b**) Quantification of the ratios for each condition. (**c**) *In vivo* 2-photon images from 3 different diabetic mice (*db/db*$^{mt\text{-}roGFP}$) per treatment group treated with saline or mitoTEMPO (10 mg/kg, 3 days, i.p.). Top panels show oxidized excitation channel, and the bottom panels display the reduced excitation channel. Bar = 25 μm. (**d**) Ratio quantification from 2-photon images. Data are presented as mean ± SEM. $^{**}P < 0.01$,$^{***}P < 0.001$. To optimize viewing of this image, please see the online version of this article at www.kidney-international.org.

(TCMK1) (Figure 4g and h). Taken together, these data suggest that bypassing electron transport in podocytes away from the dysfunctional complex I can prevent HG-induced mitochondrial ROS.

DISCUSSION

We demonstrate that the oxidation ratio of mt-roGFP is increased in the kidneys of transgenic *db/db*$^{mt\text{-}roGFP}$ diabetic mice compared with their control littermates using 2-photon microscopy in live animals. Our findings confirm those of a number of previous publications, suggesting enhanced mtROS production in DN. However, these findings are in contrast with an *in vivo* analysis of mtROS using transcutaneous fluorescent imaging post-DHE administration.[6] Possible explanations for the differences could include that different experimental models of DN were used in the 2 studies. Indeed, whereas Dugan *et al.*, used a streptozotocin model of DN for their *in vivo* studies, we used the *db/db* model in our experimental model. Furthermore, our reporter is specifically localized to mitochondria, provides a dynamic readout, and is cofactor independent.

Our findings also suggest that overcoming electron transport deficiencies at complex I using the yeast NADH-dehydrogenase Ndi1 can circumvent HG-induced mtROS in podocytes. Previous publications have indicated that Ndi1 could rescue complex I dysfunction by facilitating electron transport from NADH to coenzyme Q without generating additional ROS.[19,20] We find that bypassing complex I could improve mtROS in podocytes and tubular cells exposed to HG conditions, suggesting that complex I dysfunction is an important contributor to the increased mtROS in the HG environment.

In conclusion, our data strongly suggest that mtROS is increased under diabetic conditions in the kidney. Our approach has established a new and powerful model to monitor *in vivo* redox changes in the kidney mitochondria of diabetic mice. This model could also be used to screen the effect of targeted therapies on mtROS production in real-time and *in vivo*.

METHODS

Additional methods are available in the Supplementary Material.

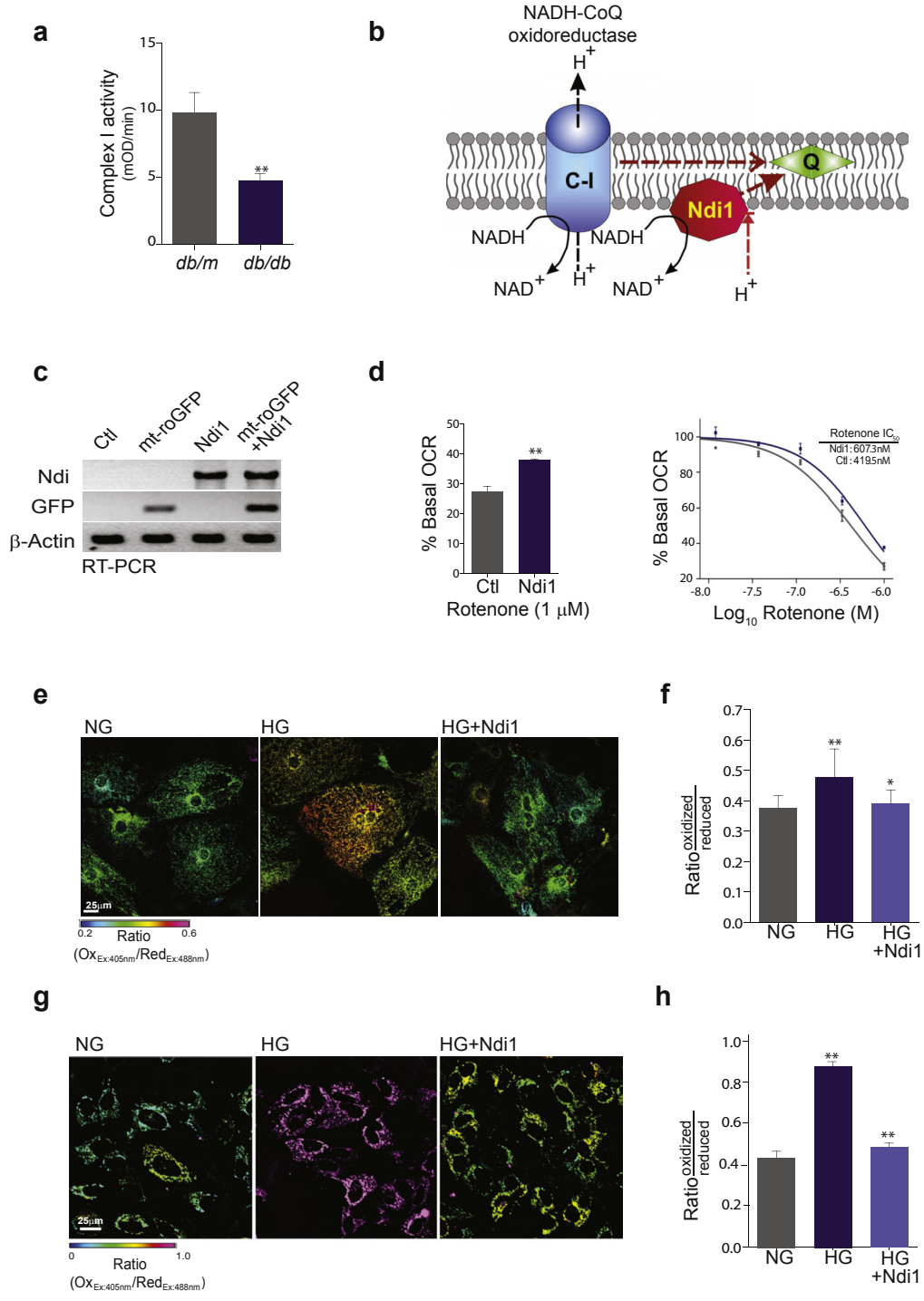

Figure 4 | Bypass of complex I electron transport prevents high glucose (HG)–induced reactive oxygen species in podocytes. (**a**) Complex I activity measurement from mitochondria of freshly isolated podocytes from 16-week-old nondiabetic (*db/m*) and diabetic (*db/db*) mice. (**b**) Cartoon of Ndi1 depicting its transport of electrons from NADH to Q while bypassing Complex I and failing to transport a proton. (**c**) Ectopic mRNA expression of roGFP and Ndi1 from stably transfected cultured podocytes. β-Actin is shown as the internal loading control for the RT-PCR. (**d**) Bar graphs represent percentage basal oxygen consumption rate (OCR) measurements of podocytes stably expressing the yeast Ndi1 construct treated with 1 μM rotenone (left). The IC_{50} of control or Ndi1 expressing podocytes was calculated following rotenone treatment ranging from 10nM to 1μM (right). (**e**) Pseudocolored ratiometric images of differentiated podocytes cultured in normal glucose (NG) or HG conditions, with and without Ndi1. Shown as a gradient of color intensity from the more reduced (blue) to the more oxidized (purple) form of mt-roGFP. Bar = 25 μm. Ratiometric color gradient values are shown. (**f**) Quantification of Ox/Red ratios from podocytes described in panel (**e**). Data are presented as mean ± SEM. $^*P < 0.05$, $^{**}P < 0.01$. (**g**) Pseudocolored ratiometric images of TCMK1 tubular cells cultured in NG or HG conditions, with and without Ndi1, shown as a gradient of color intensity from the more reduced (blue) to the more oxidized (purple) form of mt-roGFP. Bar = 25 μm. Ratiometric color gradient values are shown. (**h**) Quantification of Ox/Red ratios from podocytes described in panel (**g**). Data are presented as mean ± SEM. $^*P < 0.05$, $^{**}P < 0.01$. To optimize viewing of this image, please see the online version of this article at www.kidney-international.org.

Animal work

All animal studies were conducted according to the "Principles of Laboratory Animal Care" (NIH publication No. 85023, revised 1985) and the guidelines of the IACUC at Baylor College of Medicine and IBT/Texas A&M Health Science Center. The mt-roGFP construct and the generation of transgenic redox sensitive mt-roGFP mice have been previously described.[7] These transgenic mice were crossed to diabetic and control mice obtained from Jackson Laboratories (Bar Harbor, ME; strain: BKS.Cg-Dock7$^{m+/+}$Lepr$^{db/J}$). Resulting progeny were genotyped to verify their diabetic (*db/db*) or nondiabetic control (*db/m*) genotypes, as well as congenital acquisition of the transgenic roGFP.

Statistical analysis

All statistical analyses were performed using Prism (Graphpad Software, La Jolla, CA). Data are presented as group mean ± SEM. Statistical comparisons between 2 groups were performed using 2-tailed, unpaired Student's *t*-test. Statistical comparisons between multiple groups were performed using 1-way analysis of variance with Tukey's multiple comparison tests. *P* values less than 0.05 were considered statistically significant.

DISCLOSURE

All the authors declared no competing interests.

ACKNOWLEDGMENTS

We thank Dr. Tegy Vadakkan (Optical Imaging & Vital Microscopy Core of Advanced Core Labs at BCM, Houston, TX); and Dr. Leoncio Vergara (Center for Advanced Imaging, Texas A&M Health Science Center, Houston, TX) for providing expertise and help with 2-photon and live cell imaging. This work was supported by NIH grants R01DK091310 and R01DK078900 to FD.

SUPPLEMENTARY MATERIAL

Supplementary Methods.

Supplementary material is linked to the online version of the paper at www.kidney-international.org.

REFERENCES

1. Brownlee M. Biochemistry and molecular cell biology of diabetic complications. *Nature*. 2001;414:813–820.
2. Hou Y, Li S, Wu M, et al. Mitochondria-targeted peptide SS-31 attenuates renal injury via an antioxidant effect in diabetic nephropathy. *Am J Physiol Renal Physiol*. 2016;310:F547–F559.
3. Wang W, Wang Y, Long J, et al. Mitochondrial fission triggered by hyperglycemia is mediated by ROCK1 activation in podocytes and endothelial cells. *Cell Metab*. 2012;15:186–200.
4. Long J, Badal SS, Ye Z, et al. Long noncoding RNA Tug1 regulates mitochondrial bioenergetics in diabetic nephropathy. *J Clin Invest*. 2016;126:4205–4218.
5. Coughlan MT, Sharma K. Challenging the dogma of mitochondrial reactive oxygen species overproduction in diabetic kidney disease. *Kidney Int*. 2016;90:272–279.
6. Dugan LL, You YH, Ali SS, et al. AMPK dysregulation promotes diabetes-related reduction of superoxide and mitochondrial function. *J Clin Invest*. 2013;123:4888–4899.
7. Guzman JN, Sanchez-Padilla J, Wokosin D, et al. Oxidant stress evoked by pacemaking in dopaminergic neurons is attenuated by DJ-1. *Nature*. 2010;468:696–700.
8. Dooley CT, Dore TM, Hanson GT, et al. Imaging dynamic redox changes in mammalian cells with green fluorescent protein indicators. *J Biol Chem*. 2004;279:22284–22293.
9. Hanson GT, Aggeler R, Oglesbee D, et al. Investigating mitochondrial redox potential with redox-sensitive green fluorescent protein indicators. *J Biol Chem*. 2004;279:13044–13053.
10. Chen J, Chen JK, Harris RC. EGF receptor deletion in podocytes attenuates diabetic nephropathy. *J Am Soc Nephrol*. 2015;26:1115–1125.
11. Baynes JW. Role of oxidative stress in development of complications in diabetes. *Diabetes*. 1991;40:405–412.
12. Brownlee M. The pathobiology of diabetic complications: a unifying mechanism. *Diabetes*. 2005;54:1615–1625.
13. Coughlan MT, Thallas-Bonke V, Pete J, et al. Combination therapy with the advanced glycation end product cross-link breaker, alagebrium, and angiotensin converting enzyme inhibitors in diabetes: synergy or redundancy? *Endocrinology*. 2007;148:886–895.
14. Sourris KC, Harcourt BE, Tang PH, et al. Ubiquinone (coenzyme Q10) prevents renal mitochondrial dysfunction in an experimental model of type 2 diabetes. *Free Radic Biol Med*. 2012;52:716–723.
15. Nishikawa T, Edelstein D, Du XL, et al. Normalizing mitochondrial superoxide production blocks three pathways of hyperglycaemic damage. *Nature*. 2000;404:787–790.
16. Chouchani ET, Methner C, Nadtochiy SM, et al. Cardioprotection by S-nitrosation of a cysteine switch on mitochondrial complex I. *Nat Med*. 2013;19:753–759.
17. Wheaton WW, Weinberg SE, Hamanaka RB, et al. Metformin inhibits mitochondrial complex I of cancer cells to reduce tumorigenesis. *Elife*. 2014;3:e02242.
18. Seo BB, Kitajima-Ihara T, Chan EK, et al. Molecular remedy of complex I defects: rotenone-insensitive internal NADH-quinone oxidoreductase of Saccharomyces cerevisiae mitochondria restores the NADH oxidase activity of complex I-deficient mammalian cells. *Proc Natl Acad Sci U S A*. 1998;95:9167–9171.
19. Park JS, Li YF, Bai Y. Yeast NDI1 improves oxidative phosphorylation capacity and increases protection against oxidative stress and cell death in cells carrying a Leber's hereditary optic neuropathy mutation. *Biochim Biophys Acta*. 2007;1772:533–542.
20. Cannino G, El-Khoury R, Pirinen M, et al. Glucose modulates respiratory complex I activity in response to acute mitochondrial dysfunction. *J Biol Chem*. 2012;287:38729–38740.